

Excess Currents Larger than the Point Contact Limit in Normal Metal-Superconducting Junctions

Richard Riedel and Philip F. Bagwell
Purdue University
School of Electrical Engineering and Computer Science
West Lafayette, Indiana 47907
(June 23, 2018)

In a point contact NS junction, perfect Andreev reflection occurs over a range of voltages equal to the superconducting energy gap, producing an excess current of $I_{\text{exc}} = (4/3)(2e\Delta/h)$. If the superconductor has a finite width, rather than the infinite width of the point contact, one cannot neglect superfluid flow inside the superconducting contact. The energy range available for perfect Andreev reflections then becomes larger than the superconducting gap, since superfluid flow alters the dispersion relation inside the finite width superconductor. We find a maximum excess current of approximately $(7/3)(2e\Delta/h)$ when the width of the superconductor is approximately $7/3$ times the width of the normal metal.

I. INTRODUCTION

At a normal metal - superconductor (NS) junction, electrons incident from the normal metal can be scattered into time reversed electrons (holes) by the pairing potential. This conversion process is known as Andreev reflection.¹ When the NS junction carries an electrical current, Andreev reflection is accompanied by the conversion of normal current to supercurrent.^{2,3} This supercurrent flow modifies the current-voltage relation in NS and NSN junctions^{4,5,6}, superconducting wires^{7,8}, SNS junctions⁹, and NS junctions with a supercurrent parallel to the NS interface¹⁰. In this paper we consider the current-voltage relation for NS junctions having a supercurrent flow perpendicular to the NS junction.

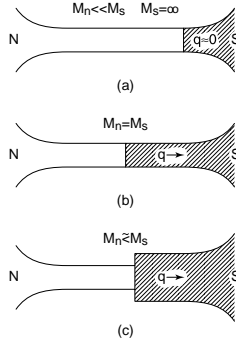


FIG. 1. Different types of NS Junctions. (a) NS point contact, (b) N-Narrow S-S, (c) N - Wider S-S. The wire width determines the number of conducting modes in the narrow segments (M_N and M_S). The superfluid flow velocity v_s cannot be neglected when $M_N \simeq M_S$.

The superfluid flow present for the point contact NS junction in Fig. 1(a) will have little effect on its I-V characteristic, since the current density inside the wide superconductor approaches zero. However, for the NS

junctions shown in Fig. 1(b)-(c), the number of conducting modes in the superconducting wire (M_S) is comparable to the number of conducting modes in the normal wire (M_N). Since the current density is not zero inside the superconductor, one cannot neglect the effect of a superfluid flow on the I-V characteristics of the NS junctions shown in Fig. 1(b)-(c). Since the superfluid flow strongly modifies the dispersion relationship of the superconductor when the ratio of the number of conducting modes $\alpha = M_S/M_N$ is of order one, including such a superfluid flow will influence the I-V characteristic of NS junctions. Since the number of conducting modes is roughly proportional to the width of the conductor, namely $\alpha \simeq W_S/W_N$, we can vary the ratio of conducting modes by varying the width of the superconductor W_S .

Blonder, Tinkham and Klapwijk (BTK) showed that the point contact NS junction in Fig. 1(a) carries a larger current than a normal metal point contact junction¹¹. This 'excess' current is due to the presence of Andreev reflection, and has the value $I_{\text{exc}} = (4/3)(2e\Delta/h)$ in a ballistic point-contact NS junction. By varying the width of the superconducting wire forming the NS junction in Fig. 1(c), we determine in this paper how the excess current varies as a function of the transverse mode ratio α . Using both an independent band model, and a second model which includes scattering between different lateral modes at the NS interface, we show the excess current in NS junction can be much larger than the BTK result. This enhancement of the excess current over the BTK value has also been noted in Ref.⁵.

More Andreev reflections can occur at higher voltages when a supercurrent flows perpendicular to the NS interface, accounting for an excess current larger than the BTK result. If the superconductor is narrower than about $W_S < (7/3)W_N$, the narrow region of the superconductor exceeds its critical current before allowing the maximum number of Andreev reflections. If the superconductor is much wider than $W_S \gg (7/3)W_N$, there is

too much geometrical dilution of the supercurrent for a significant superfluid flow to develop inside the narrowest region of the superconductor. We find a maximum excess current when the width of the superconductor is approximately $W_S = (7/3)W_N$.

II. WHY SUPERFLUID FLOW INCREASES THE EXCESS CURRENT

In this section we give the simplest physical model which illustrates why the excess current in NS junctions can be larger than the point contact limit. To make our physical points, we construct a crude two fluid model, which does not obey electrical current conservation at every point in space. A fully self-consistent solution of the Bogoliubov-deGennes equations automatically ensures current conservation, eliminating the need for this ad-hoc two-fluid model, but requires more computational effort. The two-fluid model we develop only guarantees current conservation at the terminal contacts. A fully self-consistent solution of the BdG equations in a single mode junction ($\alpha = 1$), done in section III, gives the same results for the excess current as the two-fluid model. Viewing the electrical conduction in terms of this two fluid model, therefore, allows us to obtain a value of the superfluid velocity v_s inside the superconducting contacts for each value of the bias voltage across the NS or NIS junction. We then use this value of the flow velocity v_s to compute Andreev and normal reflection probabilities for each value of the voltage, and thus obtain the electrical current in a globally self-consistent manner.

A. Two Fluid Model

Figure 2 shows the energy band diagram of an NS junction when the superconductor carries a finite supercurrent⁸. In a transmission formalism, one must compute the electrical current operator for all incident quasi-particle states, and add them to obtain the total current. Ref.¹² evaluates the electrical current operator on the normal side of the NS junction in terms of particle current transmission and reflection probabilities. The derivation in section 3 of Ref.¹² is valid for a multiple moded NS junction subject to a superfluid flow. Ref.¹² recovers the well-known BTK current formula¹¹, namely (for zero temperature)

$$I = (2e/h)M_N \int_0^{eV} [1 - T_{Ne,Ne}(E) + T_{Nh,Ne}(E)]dE. \quad (1)$$

In Eq. (1) we use the notation of Ref.¹², where the $T_{N\delta,N\beta}$ particle current reflection probabilities from the incident

channel ($N\beta$) to reflected channel ($N\delta$). The indices $\beta, \delta = e$ or h for electron-like or hole-like quasi-particles. We must compute the both the normal $T_{Ne,Ne} = R_N$ and Andreev $T_{Nh,Ne} = R_A$ reflection probabilities when the superconducting contact is subject to a superfluid flow. For simplicity we have taken the M_N modes in the normal conductor to be both independent and to carry identical electrical currents.

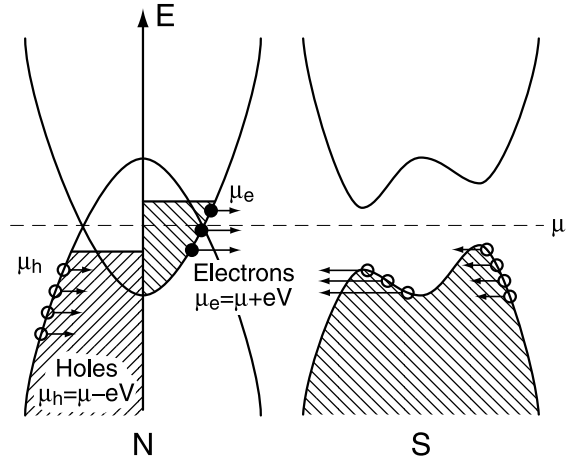


FIG. 2. Energy band diagram of an NS junction subject to a superfluid flow $v_s \geq 0$. The shifted energy bands in the superconductor cause Andreev reflection to occur at higher energies than without superfluid flow. The contacts inject electron-like (solid dots) and hole-like (open circles) quasi-particles as shown.

In order for the superconductor to carry a finite supercurrent, the form of the order parameter $\Delta(x)$ inside the superconductor must be generalized to $\Delta(x) = |\Delta|e^{2iqx}$. The superfluid velocity is $v_s = \hbar q/m$. If we consider solutions accurate within the Andreev approximation ($|E| \ll \mu$), we can approximate the dispersion relation near the Fermi level as being rigidly shifted in energy as⁸

$$\frac{\hbar^2 k^2}{2m} - \mu \simeq \pm \sqrt{(E \mp |\Delta|(q/q_d))^2 - |\Delta|^2}. \quad (2)$$

Here $v_d = \hbar q_d/m = |\Delta|/\hbar k_F$ is the Landau depairing velocity.¹³ The electrical current is given by $I_C \simeq env_s M_S$ with $n = 2(k_F/\pi)$ the electron density per mode and M_S the number of (equivalent, for simplicity) conducting modes in the superconductor⁷. We can rewrite the supercurrent I_C in terms of the depairing velocity as

$$I_C \simeq (4e|\Delta|/\hbar)(v_s/v_d)M_S. \quad (3)$$

At zero temperature, the critical current phase boundary occurs when $v_s = v_d$. We must therefore maintain $v_s < v_d$ to preserve the superconducting order parameter $|\Delta| \neq 0$.

Inside the superconductor, the electrical current is often argued to be composed of a ‘quasi-particle’ and ‘condensate’ contribution^{11,14}. To break Eq. (1) down into

these two contributions to the current we use the sum rule¹¹

$$1 = T_{Ne,Ne}(E) + T_{Nh,Ne}(E) + T_{Se,Ne}(E) + T_{Sh,Ne}(E). \quad (4)$$

Equation (4) states that the normal ($T_{Se,Ne} = T_N$) and Andreev ($T_{Sh,Ne} = T_A$) particle current transmission coefficients into the superconductor conserve the total number of quasi-particles. Combining Eqs. (1) and (4), the electrical current inside the superconductor at zero temperature is

$$I = I_{QP} + I_A. \quad (5)$$

We identify the portion of the electrical current due to ‘quasi-particle’ injection as

$$I_{QP} = (2e/h)M_N \int_0^{eV} [T_{Se,Ne}(E) - T_{Sh,Ne}(E)]dE, \quad (6)$$

and the ‘Andreev’ portion of the current I_A as

$$I_A = (2e/h)M_N \int_0^{eV} 2[T_{Nh,Ne}(E) + T_{Sh,Ne}(E)]dE. \quad (7)$$

The ‘Andreev’ current in Eq. (7) equals twice the sum of all Andreev processes.

Equations (5)-(7) give the same current as the BTK expression from Eq. (1), since both are simply the current operator evaluated inside the normal metal. The key physical element in our ‘two-fluid’ model is that we require that both Eqs. (3) and (7) for the ‘condensate’ current I_C and the ‘Andreev’ current I_A must be equal. We examine this assumption more rigorously in the Appendix, by evaluating the electrical current operator inside the superconductor. In this section we make a plausibility argument for equating I_A from Eq. (7) with the ‘condensate current’ I_C from Eq. (3), or the ‘current of Cooper pairs’.

Eq. (7) expresses the condensate current in terms of probabilities for Andreev reflection and Andreev transmission of an electron incident from the normal metal. Conversely, Eq. (3) expresses the condensate current in terms of the superfluid velocity. That an incident electron and a reflected hole on the normal metal side requires a Cooper pair to move off into the superconductor (to preserve electrical charge conservation) is well known¹¹. Similarly, Andreev transmission of an electron also requires a Cooper pair flow inside the superconductor. Andreev reflection and Andreev transmission of electrons incident from the normal metal require Cooper pairs flow away from the NS interface (in the same direction) for both processes. Equation (7) embodies this physical reasoning. Similarly, identifying Eq. (6) as the ‘quasi-particle’ contribution to the electrical current is also quite natural, being proportional to the electrical current operator for an electron injected from the normal metal (evaluated on the superconducting side).

The ‘two fluid’ picture here requires Eqs. (3) and (7) be equal be satisfied in order to guarantee global current conservation. Once the junction geometry and applied voltage is specified, the only free parameter in Eqs. (3) and (7) is the superfluid velocity $v_s = \hbar q/m$. Since the quasi-particle transmission and reflection coefficients themselves depend on v_s , equating Eqs. (3) and (7) is then a globally self-consistent procedure for determining the superfluid flow velocity v_s . Using this value for v_s , one then uses either Eq. (1) or (5) to find the terminal currents for each value of the bias voltage V .

B. Two-Fluid Approximation for Ballistic NS Junction

We now restrict our attention to ballistic NS junctions, and approximate the energy bands near the Fermi level as simply rigidly shifted in energy by an amount $\pm|\Delta|(v_s/v_d)$, as determined from Eq. (2). When the superconductor carries a finite supercurrent, we can then obtain the Andreev reflection coefficient from

$$T_{Nh,Ne}(E) = R_A^0(E - |\Delta|(v_s/v_d)). \quad (8)$$

Here $R_A^0(E)$ is the Andreev reflection coefficient found by BTK¹¹ when the superfluid flow is zero ($v_s = 0$), namely

$$R_A^0(E) = \begin{cases} 1 & |E| \leq |\Delta| \\ \left(\frac{E - \sqrt{E^2 - |\Delta|^2}}{E + \sqrt{E^2 - |\Delta|^2}} \right) & |E| \geq |\Delta| \end{cases}. \quad (9)$$

This rigid shift in the Andreev reflection coefficient, corresponding to the rigid shift in the energy bands near the Fermi level, is shown in Fig. 3. Simply shifting the reflection coefficients in energy is not a valid approximation when a tunnel barrier is present at the NS interface¹⁵, as also noted in Fig. 3. Since the differential conductance of an NS junction is

$$\left. \frac{dI}{dV} \right|_V = \frac{2e}{h} [1 + R_A(E = eV) - R_N(E = eV)], \quad (10)$$

a differential conductance measurement producing a larger than expected energy gap could point to significant superfluid flow in the junction.

Shifting the Andreev reflection coefficient in energy makes it possible for the ‘negative energy’ Andreev reflections, i.e. the Andreev reflection probabilities having $E < 0$ in Eqs. (9) to contribute to the excess electrical current. These ‘negative energy’ Andreev reflections are shown as the additional area under the Andreev reflection probability for $E > 0$ when $v_s > 0$ in Fig. 3. At zero temperature, Eqs. (1) and (8) give

$$I = (2e/h)M_N \int_0^{eV} [1 + R_A^0(E - |\Delta|(v_s/v_d))]dE. \quad (11)$$

To determine the superfluid velocity v_s in Eq. (11), Eqs. (3) and (7) require

$$|\Delta|\alpha(v_s/v_d) = \int_0^{eV} R_A^0(E - |\Delta|(v_s/v_d))dE. \quad (12)$$

Equation (12) is a self-consistent equation for the superfluid velocity v_s , and depends on the ratio of the number of conducting modes in the superconductor to the normal conductor $\alpha = M_S/M_N$. The largest possible excess current would occur if we could fix $v_s \rightarrow \infty$ in Eqs. (11), and would give twice the BTK result of $I_{\text{exc}}^{\text{max}} = 2I_{\text{exc}}^{\text{BTK}} = (8/3)(2e\Delta/h)$. However, this theoretical maximum excess current is not possible due to the constraint that the superfluid velocity must remain smaller than the depairing velocity. One must therefore discard any solution of Equation (12) giving $v_s > v_d$.

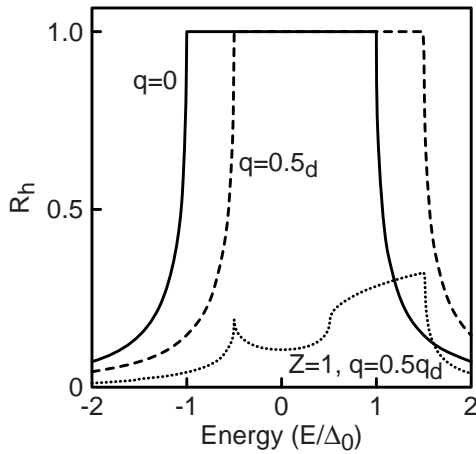


FIG. 3. Andreev reflection probability for an electron incident on an NS interface when the superfluid velocity is zero (solid line) and when $v_s = v_d/2$ (dashed line). Superfluid flow simply shifts the Andreev reflection probability by an amount $\Delta(v_s/v_d)$. If a tunnel barrier is placed at the NS interface (dotted line), there is no simple relation between the Andreev reflection probabilities with and without superfluid flow.

C. Numerical Evaluation of Two-Fluid Formula

We plot the numerical solution of Eqs. (11)-(12) for the total current through the NS junction as a function of the voltage in Fig. 4. When the transverse mode ratio is small, namely when $\alpha \leq 7/3$ shown in Fig. 4(a), there is a voltage above which current conservation requires that v_s exceed the Landau depairing velocity of the superconductor. When $v_s \geq v_d$, the narrower superconducting region (between the large normal contact and the large superconducting reservoir) becomes a normal conductor. This collapse of the order parameter in the narrower superconducting wire continues until a new NS

interface is formed where the narrow conductor meets the wide superconducting reservoir. Geometrical dilution of the supercurrent where the superconductor widens into a thermodynamic reservoir moves the NS interface so that a stable point contact junction is formed. Forcing the narrower superconducting region into the normal state therefore creates a point contact NS junction having $\alpha = \infty$, i.e. the BTK limit of an NS junction. Forcing the narrower superconducting region to become normal therefore forces the excess current to fall abruptly to the BTK limit shown in Fig. 4(a).

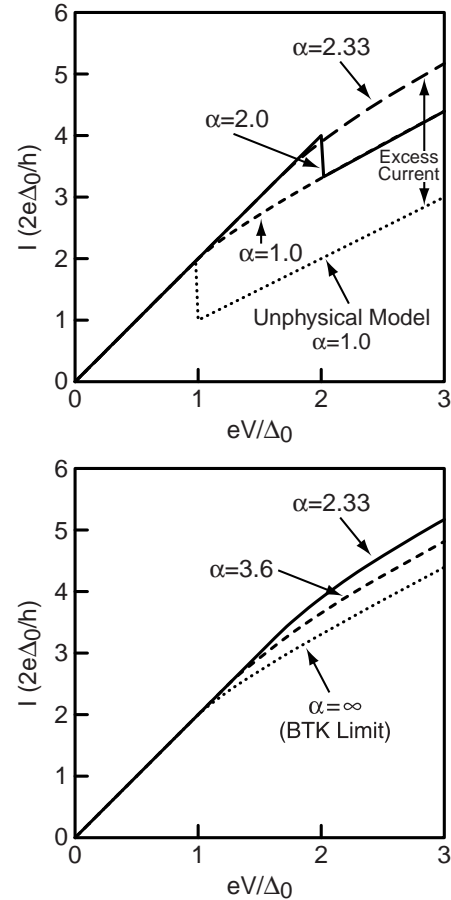


FIG. 4. (a) When the transverse mode ratio $\alpha < (7/3)$, the order parameter in the narrow superconducting wire can collapse, giving rise to discontinuities in the I-V relation. (b) When $\alpha > (7/3)$ no such discontinuities arise. The excess current is larger than the BTK result for $\alpha = 7/3$, shown in both (a) and (b). The I-V evolves smoothly into the BTK result for a point contact NS junction when $\alpha \rightarrow \infty$.

An excess current larger than the BTK limit is also shown in Fig. 4(a), due to the additional ‘negative energy’ Andreev reflections. When the transverse mode ratio is larger, namely when $\alpha \geq 7/3$ shown in Fig. 4(b), the superfluid velocity in the narrower superconductor is always less than the Landau depairing velocity. Consequently, no abrupt drops in the current occur for any

value of the voltage. The excess current simply decreases gradually from its maximum value at $\alpha = 7/3$ to the BTK value for a NS point contact at $\alpha = \infty$.

We plot the maximum excess current in a ballistic NS junction versus the mode ratio α in Figure 5. The excess current at any given voltage is defined as the difference between the current carried by the NS superconducting junction and a normal NN junction, namely $I_{ex}(V) = I_{NS}(V) - I_{NN}(V)$. The maximum excess current occurs at voltage for which $I_{ex} = \text{Max}[I_{ex}(V)]$. For $\alpha < 4/3$ the excess current is given by the point contact value, namely the BTK result of $(4/3)(2e\Delta/h)$, and occurs at a voltage $V = \infty$. When $4/3 \leq \alpha \leq 7/3$ the excess current occurs at a finite voltage $V \leq \infty$, and is larger than the BTK result. As the transverse mode ratio increased above $\alpha \geq 7/3$, geometrical dilution of the supercurrent reduce the band tilting in the superconductor, reducing the maximum excess current of the junction. When the mode ratio is very large, so that $\alpha \rightarrow \infty$ we recover the point contact result for the excess current.

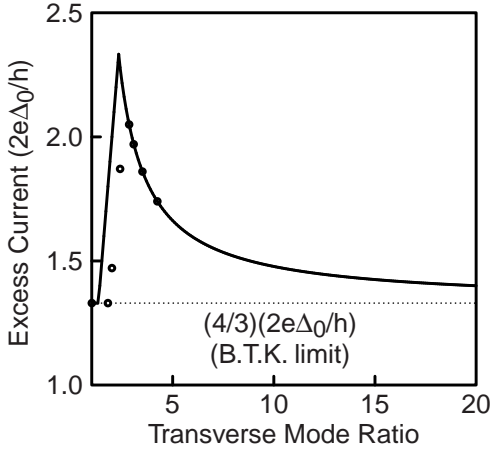


FIG. 5. The excess current I_{exc} of a ballistic normal-superconducting wire at zero degrees Kelvin is maximum when the transverse mode ratio is $\alpha = (M_S/M_N) = 7/3$. I_{exc} approaches the point contact (BTK) value of $4/3(2e\Delta/h)$ when $\alpha \rightarrow \infty$. Collapse of the order parameter in the narrow superconducting wire limits I_{exc} when $\alpha < 7/3$.

The circled dots in Figure 5 show the results of a more realistic numerical calculation¹⁵ for the excess current. As detailed in Ref.¹⁵, we permit interband scattering at the NS junction and allow different conducting modes in the superconductor to carry different amounts of supercurrent⁷. The general behavior for the excess current versus mode ratio α of this more realistic NS junction model is quite similar to our simplified model, except the maximum in the excess current is slightly smaller and shifted to a slightly larger transverse mode ratio. The slightly lower excess current arises because the higher lying modes have a smaller Fermi velocity, and therefore the Andreev reflection coefficients for the higher lying modes do not shift in energy as much as the lower ly-

ing modes. We conclude that this more realistic model, even though still a two-fluid type model which only globally conserves electrical current, confirms the essential features of our simpler independent mode calculation in this section.

D. Limiting Cases of Two-Fluid Formula

We can understand how the excess current I_{exc} depends on the mode ratio $\alpha = M_S/M_N$ in Figure 5 by examining Eqs. (11)-(12) in different limits. The integral of the shifted Andreev reflection probability in Eqs. (11)-(12) can be done analytically to yield

$$\int_0^{eV} R_A^0(E - |\Delta|(v_s/v_d))dE = eV \quad (13)$$

when $eV \leq |\Delta|(1 + (v_s/v_d))$. In this limit, Eqs. (12) and (13) show the superfluid velocity increases linearly with bias voltage V . For larger biases, namely when $eV \geq |\Delta|(1 + (v_s/v_d))$, the superfluid velocity increases more slowly with voltage, as determined from

$$\begin{aligned} \int_0^{eV} R_A^0(E - |\Delta|(v_s/v_d))dE \\ = |\Delta|(1 + (v_s/v_d)) + |\Delta|[\frac{1}{3} - \frac{1}{2}e^{-\gamma} + \frac{1}{6}e^{-3\gamma}]. \end{aligned} \quad (14)$$

The factor γ in Eq. (14) is

$$\gamma = \cosh^{-1}(\frac{eV}{|\Delta|} - \frac{v_s}{v_d}). \quad (15)$$

The excess current we obtain from

$$I_{exc} = (2e/h)M_N \int_0^{eV} R_A^0(E - |\Delta|(v_s/v_d))dE. \quad (16)$$

Consider first the case where the narrower superconducting wire is not driven normal, so that $v_s < v_d$ for all values of voltage. In that case, the maximum excess current occurs when $V = \infty$, so that $\gamma = \infty$ in Eq. (15). Eqs. (12) and (14) for the superfluid velocity then reduce to $(\alpha - 1)(v_s/v_d) = 4/3$. The maximum allowed superfluid velocity, $(v_s/v_d) = 1$, then occurs for a transverse mode ratio of $\alpha = 7/3$. The excess current from Eqs. (16) and (14) then becomes

$$I_{exc} = \left(\frac{2e|\Delta|}{h}M_N\right) \left(\frac{4}{3}\right) \left(\frac{\alpha}{\alpha - 1}\right), \quad (17)$$

when $\alpha \geq 7/3$. The excess current reaches its maximum value of $I_{exc} = (7/3)(2e|\Delta|/h)M_N$ when $\alpha \geq 7/3$ as shown in Figure 5. Taking the limit $\alpha \rightarrow \infty$ in Eq. (17) recovers the BTK result $I_{exc} = (4/3)(2e|\Delta|/h)M_N$.

We can also obtain an analytical solution for the excess current using Eqs. (12) and (13) to determine the

superfluid velocity as $(v_s/v_d) = eV/|\Delta|\alpha$. The excess current then follows from Eqs. (16) and (13) as $I_{exc} = (2e|\Delta|/h)M_N|\Delta|\alpha(v_s/v_d)$. Using the maximum allowed depairing velocity of $(v_s/v_d) = 1$ then gives

$$I_{exc} = \left(\frac{2e|\Delta|}{h} M_N \right) \alpha. \quad (18)$$

The range of allowed mode ratios α for which Eq. (18) is valid lie along the curve $(v_s/v_d) = 1 = eV/|\Delta|\alpha$. Furthermore, Eq. (13) is only valid for $eV/|\Delta| \leq (1 + (v_s/v_d))$. Combining all these requirements restricts the mode ratio between $1 \leq \alpha \leq 2$. However, for $1 \leq \alpha \leq 4/3$ the order parameter in the narrower superconducting wire collapses before the excess current reaches the BTK value. Eq. (18) therefore describes the excess current between $4/3 \leq \alpha \leq 2$ as shown in Figure 5.

III. EXACT SOLUTION OF A SINGLE MODE NS JUNCTION

In this section we wish to evaluate several assumptions made in the two fluid model of section II. To do this, we solve the BdG equation, together with the self-consistency requirement for the order parameter, in a single band (1D) model of the NS junction where $M_N = M_S = 1$ ($\alpha = 1$). This self-consistent solution allows us to demonstrate how the supercurrent flow develops naturally from a self-consistent solution of the NS junction under a voltage bias. We use this solution to verify the approximate (two-fluid) procedure we use to guarantee global current conservation in section II. One might expect that conserving the current only globally certainly gives qualitatively correct answers for the I-V characteristic. However, since the Andreev reflection probability does not vary much (as a function of energy) if we allow the order parameter to reach its final self-consistent form, the two-fluid model also gives accurate quantitative estimates for the I-V relation.

Our self-consistent solution of the BdG equations in this section verifies the main assumptions used in our two-fluid model (when $\alpha = 1$). When a voltage is applied to the ballistic NS junction, the magnitude of $\Delta(x)$ remains approximately constant inside the superconductor (at zero temperature). However, the order parameter phase varies approximately linearly inside the superconducting metal. There are essentially no additional quasi-particles injected into the single mode NS junction at zero temperature, so the total current is simply $I = env_s$. The slope of the phase is related to the supercurrent velocity as $d\phi/dx = 2q = 2v_s m/\hbar$. The superfluid velocity is linearly related to the voltage as $I = (4e^2/h)V = env_s$. As voltage bias increases, the slope of the phase $d\phi/dx$ increases until the superfluid velocity reaches the Landau depairing velocity, $v_s = v_d$

(or $d\phi/dx = 1/\xi_0$). At this voltage $V = V_c$ the ordering parameter inside the narrow superconductor collapses, and a stable point contact NS junction forms inside the wide superconducting reservoir.

A. Self-Consistent Solution Procedure for BdG Equation

The motion of quasi-particles in our one band NS junction, including the superfluid flow inside in the superconductor, is determined from the 1D time independent Bogliobov-de Gennes¹⁶ (BdG) equation

$$\begin{pmatrix} H(x) - \mu & \Delta(x) \\ \Delta^*(x) & -(H^*(x) - \mu) \end{pmatrix} \begin{pmatrix} u(x) \\ v(x) \end{pmatrix} = E \begin{pmatrix} u(x) \\ v(x) \end{pmatrix} \quad (19)$$

The one-electron Hamiltonian $H(x)$ in Eq. (19) is

$$H(x) = -\frac{\hbar^2}{2m} \frac{d^2}{dx^2} + V(x). \quad (20)$$

The order parameter $\Delta(x)$ in Eq. (19) is given by

$$\begin{aligned} \Delta(x) &= g(x)F(x) \\ &= g(x) \sum_{pn} v_{pn}^*(x) u_{pn}(x) f_{pn} \theta(|E_{pn}| - \hbar\omega_D), \end{aligned} \quad (21)$$

where $g(x)$ is the electron-phonon interaction strength at each point and $F(x)$ is the pair correlation function. (Although we assume $g(x)$ is local, in reality it is spread over a correlation distance v_F/ω_D .) The index p in Eq. (21) denotes the lead from which the scattering state originates, namely $p = N$ is the left lead and $p = S$ the right lead. The index n in Eq. (21) denotes the good quantum numbers in the lead, namely $n = (k, \beta)$ where k is the wavenumber and $\beta = (e, h)$ the electron-like and hole-like states. The sum in Eq. (21) runs over states injected from the leads, including both positive ($E_n > 0$) and negative energies ($E_n < 0$). The coherence factors $u(x)$ and $v(x)$ in Eq. (21) are functions of the order parameter $\Delta(x)$ through Eq. (19).

In this section we show the self-consistent solutions of Eq. (19) and (21) for a voltage-biased NS junction. Details of the self-consistent solution procedure are given in Ref.⁹. To solve the order parameter self-consistently, we first assure an initial or zeroth order guess $\Delta_0(x)$ for the order parameter. We then divide the one dimensional space into differential elements, where the magnitude of the order parameter superfluid velocity are constant in each section. We match the wavefunctions and their derivatives at each interface to obtain the zeroth order wavefunctions $u_0(x)$ and $v_0(x)$. The first iteration for the order parameter $\Delta_1(x)$ we then obtain from Eq. (21) using the zeroth order wavefunctions $u_0(x)$ and $v_0(x)$, etc. The zeroth order guess for the order parameter $\Delta_0(x)$ can either be constant, i.e. $\Delta_0(x) = \Delta$, or it can contain

a superfluid flow, i.e. $\Delta_0(x) = \Delta e^{2iqx}$. Given the same electrical current flow, either initial guess for the order parameter converges to the same final answer.

The voltage bias across the NS junction is a boundary condition which determines the Fermi occupation probabilities f_{pn} in Eq. (21). The occupation probability f_{pn} of a scattering state (p, n) which originates inside the normal or superconducting reservoir p , is the same for holes and electrons when the applied bias is zero ($V = 0$). Under a voltage bias, however, electrons in the normal metal are occupied up to an energy $\mu + eV$, while holes are occupied up to an energy $\mu - eV$.¹² These different Fermi factors electron-like and hole-like quasi-particles injected from the normal metal are shown schematically in Fig. 2. The unequal occupation probabilities for holes and electrons injected from the normal metal causes these two classes of scattering states to contribute differently to the sum in Eq. (21) under an applied bias. We can write the Fermi factors as

$$f_{pn} = f_{p\beta} = f(E - eV_{p\beta}), \quad (22)$$

where $f(E) = 1/[1 + \exp(E/k_B T)]$. Here $eV_{p\beta}$ is effective biasing voltage (or effective electrochemical potential) applied to the $(p\beta)$ th lead, namely¹²

$$V_{Ne} = V, \quad (23)$$

$$V_{Nh} = -V. \quad (24)$$

In this paper the superconducting leads are grounded so that $V_{S\beta} = 0$.

To obtain the electrical current $I(x)$, we do not invoke any ad hoc ‘source term’ as done in Ref.¹¹, but instead simply evaluate the electrical current operator for a scattering state originating in lead q (having quantum number n) and terminating in lead p , namely

$$I_q = \sum_{pn} (J_u + J_v)_{q;pn} f_{pn} - \sum_{pn} (J_v)_{q;pn}. \quad (25)$$

The J_u and J_v are Schrödinger currents associated with the waves u and v , namely $J_u = (e\hbar/m)\text{Im}\{u^*(x)\nabla u(x)\}$ and $J_v = (e\hbar/m)\text{Im}\{v^*(x)\nabla v(x)\}$. The ‘vacuum current’ due to the filled hole band is argued in Ref.¹² to be zero, namely $\sum_{qn} (J_v)_{p;qn} = 0$, as we have confirmed for the NS junction. Solving Eq. (19) together with Eq. (21) guarantees electrical current conservation^{2,3,8,17,18}, even when the superconductor is far from equilibrium. A proof of this statement for NS junctions follows from generalizing the discussion in Appendix B of Ref.⁸ to the nonequilibrium case. If the nonequilibrium system involves two superconductors at different biases¹⁹, current conservation is more complex and $\sum_{qn} (J_v)_{p;qn} \neq 0$.

B. Order Parameter Phase

Consider first the NS junction, where the coupling constant $g(x)$ is

$$g(x) = \begin{cases} g_R & x > 0 \\ 0 & x < 0 \end{cases} \quad (26)$$

We choose g_R and ω_D so that the critical temperature of the right superconductor is $T_c = 6.6\text{K}$. Our initial guess for the order parameter we take to be

$$\Delta_0(x) = \begin{cases} \Delta & x > 0 \\ 0 & x < 0 \end{cases} \quad (27)$$

We therefore do not force a superfluid flow inside the superconductor from our zeroth order guess for the order parameter.

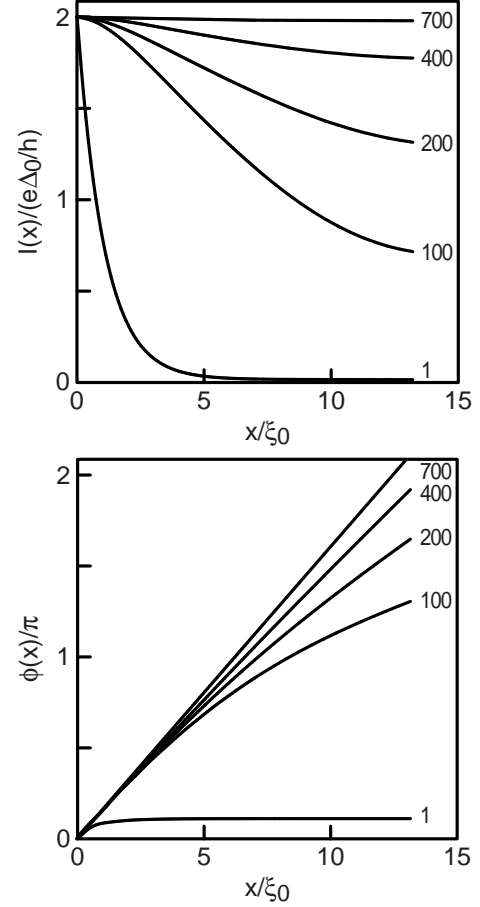


FIG. 6. Both (a) the electrical current throughout an NS junction, and (b) the phase in the superconducting metal, develop naturally from a self-consistent model. The initial order parameter guess $\Delta_0(x)$ assumed zero supercurrent, however a superfluid flow appeared naturally upon reaching self-consistency.

Fig. 6(a) shows the electrical current $I(x)$ versus position x inside the superconductor. The numbers beside the lines in Fig. 6(a) denote the iteration number. For the first iteration ($N = 1$), the electrical current dies off within a coherence length of the NS interface, so that the electrical current is not conserved. After the iterative scheme converges ($N = 700$) in Fig. 6(a), we see the electrical current $I(x)$ is constant as a function of position,

indicating the electrical current is indeed conserved. In Fig. 6(b) we plot the order parameter phase inside the superconductor as a function of position. A uniform phase gradient develops inside the superconductor when the iterative scheme has converged to self-consistency, showing that the development of a supercurrent is necessary to guarantee current conservation. We expected this constant order parameter phase gradient in the NS junction, since it is similar to that constant order parameter phase found in the self-consistent solution of the SNS junction.⁹

We can understand these results using our two-fluid picture from section II, and assuming rigidly shifted energy bands. The maximum current of $4e\Delta/h$ is reached when the voltage $eV = \Delta$. At this point the energy bands have shifted up faster than the Fermi level of the normal contact, and thus no direct transmission of electrons across the junction inside the energy range $0 < E < eV$ is allowed. Andreev transmission will also be small, as is usually the case in NS junctions. There will therefore be essentially no quasi-particles above the Fermi level of the superconductor, while all states below the Fermi level are filled. The quasi-particle contribution to the current inside the superconductor, I_{QP} in Eq. (6), is essentially zero in the single mode NS junction when $eV < \Delta$. The electrical current is therefore $I = env_s$ in this single moded NS junction, the same as for a uniform 1D superconductor. The order parameter magnitude collapses when the superfluid velocity equals the depairing velocity $v_s = v_d$, at a bias voltage $eV = \Delta$.

C. Order Parameter Magnitude

Fig. 7(a) shows the magnitude of the condensation amplitude $F(x)$ as a function of position in both the normal and superconducting metal at zero temperature. The solid line indicates a bias voltage of $V = 0$, while the dashed line is for a bias voltage $V = 0.95V_c$ ($v_s = 0.95v_d$). The general form of the condensation amplitude $F(x)$ for a ballistic NS junction at equilibrium is well known from earlier non-self-consistent models.^{20,21} We find substantial agreement between these earlier results and our fully self-consistent calculations. In the superconductor, $F(x)$ is suppressed from its bulk value near the NS interface. In the normal metal, $F(x)$ shows behavior quite similar to the low temperature experimental results of Mota²². The dotted line in Fig. 7(a) is $F(x) \propto 1/(|x| + x_0)$, found experimentally by Mota²². The value of x_0 used in Fig. 7(a) is $x_0 = \xi_0$. The fit between the experimental determined form $F(x) \propto 1/(|x| + x_0)$ and the results of our self-consistent calculation is quite good. The result $F(x) \propto 1/(|x| + x_0)$ for the pair correlation function at low temperature in an NS junction at equilibrium ($V = 0$) was also pointed out by Falk²¹ for the asymptotic limit $x \rightarrow \infty$.

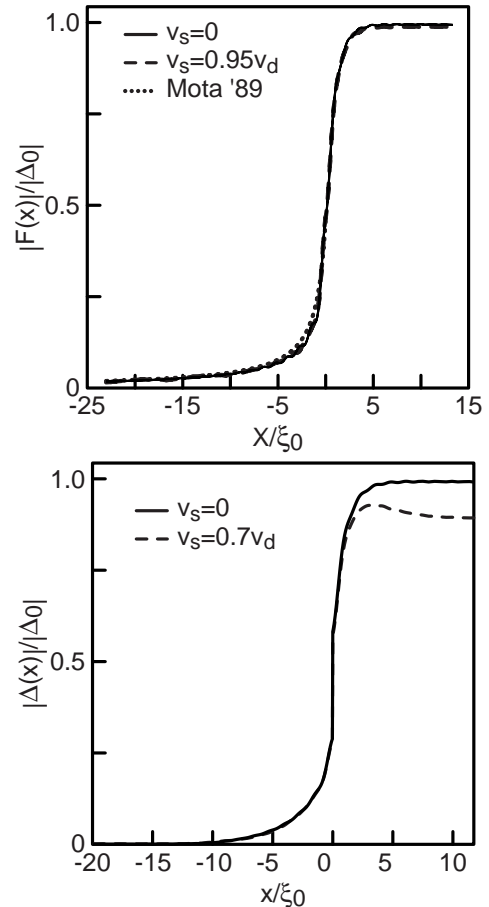


FIG. 7. The magnitude of the coherence function $F(x)$ (a) changes little when a large flow is present in a NS junction with an applied voltage. The solid line is $F(x)$ when the applied voltage is zero. When the applied voltage is large $.95\Delta$ $F(x)$ shows little change (dashed line) from the junction in equilibrium. [The phase of $F(x)$ changes linearly with position throughout the NS junction.] (b) In an S'S junction at a temperature above the critical temperature of S', the order parameter is non-zero in the "normal" metal. The finite temperature in combination with a moderate supercurrent causes a suppression of the larger gap superconductor. (dashed line)

In an NS junction, the ordering parameter $\Delta(x)$ vanishes in the normal metal because the electron-phonon coupling constant $g(x)$ is zero there. For a finite ordering parameter $\Delta(x)$ to exist inside the normal metal we must have $g(x) \neq 0$ in the normal metal. One way to achieve a non-zero $g(x)$ in the normal metal is to fabricate an S'S junction, where the superconductor S' has a smaller critical temperature than S. If we then elevate the temperature so that $T_c > T > T'_c$, we effectively form an NS junction where $g(x)$ is not zero inside the normal metal. Fig. 7(b) shows a self-consistent calculation for an such S'S junction, where $T_c = 6.6K$, $T'_c = 0.66K$, and $T = 2K$. Unlike the NS junction, where $\Delta(x) = 0$ inside the normal metal, we see a non-zero 'tail' of the ordering parameter extending into the normal metal in Fig. 7(b). At zero temperature, the bulk value

of the order parameter inside the weaker superconductor is $\Delta'(T=0) = 0.1\Delta(T=0)$. From Fig. 7(b) we see that $\Delta(x=0, T=2K) \simeq 2.5\Delta'(T=0)$, larger than even the bulk value of the order parameter in the weaker superconductor at zero temperature. When a voltage is applied to the $S'S$ junction, namely $eV = .7\Delta_0$ in Fig. 7(b), the ordering parameter inside S is now suppressed from its bulk value at $T = 2K$. This degradation of the order parameter at finite temperature, when the superconductor carries a finite supercurrent, is similar to that of a bulk superconducting wire⁸. The tail of the ordering parameter extending into S' is only slightly changed in the presence of the supercurrent.

D. Local Density of States

In addition to the magnetic susceptibility techniques used by Mota, which explore the condensation amplitude $F(x)$ in the normal metal, another method to experimentally investigating how the ordering parameter $\Delta(x)$ varies near NS interfaces is tunnelling spectroscopy using an STM tip.²³ We expect that a measurement of the differential conductance dI/dV at the STM tip is proportional to the local density of states $N(x, E)$. We can calculate the local density of states using the equation

$$N(x, E) = \frac{1}{\pi} \sum_{p,n} |u_{p,n}(x, E)|^2 + |v_{p,n}(x, E)|^2 \left| \frac{dk}{dE} \right|, \quad (28)$$

where p is the lead index and the quantum number $n = (k, \beta)$. Fig. 8(a) shows the local density of states for an NS junction having an applied voltage of $eV = .7\Delta_0$. At this bias voltage, the superconductor carries a supercurrent of $v_s = 0.7v_d$. The solid line shows $N(x, E)$ at a position $x = 5\xi_0$ inside the superconductor. The original peak in the density of states, which occurs at $E = \Delta$ when the superfluid flow $v_s = 0$, splits into two separate peaks. As the energy bands inside the superconductor tilt under the superfluid flow, the band edges move to the energies $E = [1 \pm (v_s/v_d)]\Delta$, as do the peaks in the density of states. In the normal metal, the density of states is approximately constant for energies of interest. The constant density of states in the normal metal is due to a zero pairing potential $\Delta(x) = 0$ inside the normal metal, since $g(x) = 0$ in the normal metal.

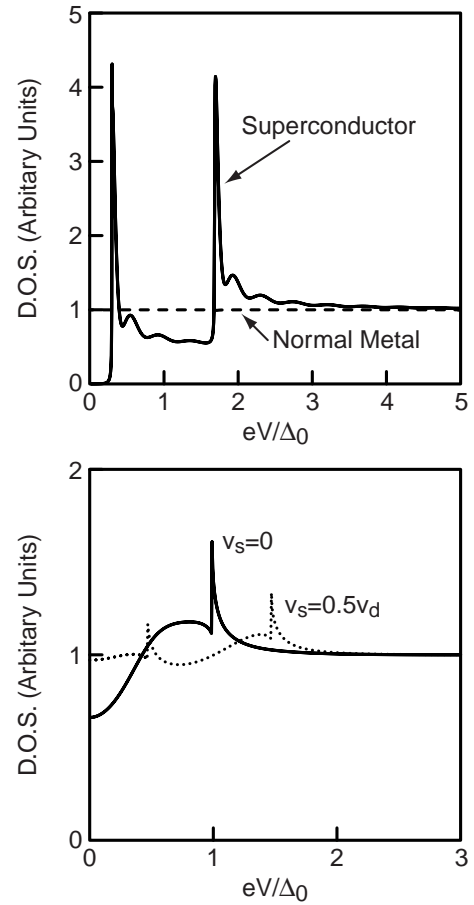


FIG. 8. (a) When a supercurrent is present in an NS junction, the local density of states inside the superconductor shows two peaks. The local density of states inside the normal conductor is constant for all $x < 0$, indicating the lack of any energy gap due to the proximity effect. (b) In an $S'S$ junction when a supercurrent is present, where S' is a superconductor above its transition temperature, structure is seen in the local density of states inside the "normal" S' metal.

Fig. 8(b) shows the local density of states for an $S'S$ junction having $T_c > T > T'_c$. We evaluate the local density of states at a position $x = -\xi_0$ in the normal metal. The local density of states inside the stronger superconductor is approximately the same as Fig. 8(a). For the two different applied voltages, where $v_s = 0$ (solid) and $v_s = .5v_d$ (dotted), the presence of the superconductor changes the density of states inside the normal metal. For $v_s = 0$, there is a depression in the density of states near $E = 0$, showing the partial development of an energy gap inside the normal metal. The density of states does not go to zero at $E = 0$, since quasi-particles incident from the left contact can still propagate to the position $x = -\xi_0$. As the current increases, the density of states inside the normal metal becomes flatter due to injection of quasi-particles from the tilted energy bands inside the superconductor. The two small peaks at $eV = .5\Delta_0$ and $eV = 1.5\Delta_0$ when $v_s = .5v_d$ are again associated with the tilted energy bands inside S , and are significantly broad-

ened by thermal smearing at $T = 2K$ (which we have ignored in Fig. 8(b)).

To summarize, while looking to justify our two-fluid model for the effect of superfluid flow in an NS junction, we studied the pair correlation function $F(x)$ and ordering parameter $\Delta(x)$. We looked at $F(x)$ and $\Delta(x)$ inside both (1) an NS junction at temperature $T = 0$, and (2) an S'S junction at a temperature $T_c > T > T'_c$. Here S' is a superconductor having an order parameter smaller than S, so that $T'_c < T_c$. The S'S junction at this temperature is therefore a type of NS junction. First, the condensation amplitude is $F(x) \simeq x_0/(|x| + x_0)$, approximately independent of the applied voltage. Second, at the voltage $V_c = \Delta_0/e$, the ordering parameter of the superconductor collapses, i.e. $\Delta_0 \rightarrow 0$. The supercurrent carried inside the superconductor at a voltage $V = V_c$ is approximately equal to the Landau depairing current $I_C = env_d$. Third, we show how the supercurrent changes the 1-D local density of states per unit energy $N(x, E)$ at various points in the normal and superconducting metals, both for the NS junction and the S'S junction. The local density of states shows the influence of the superfluid flow.

E. Locally (But Not Globally) Gapless Superconductivity

The phase gradient of $F(x)$ is approximately constant for both the NS junction in Fig. 7(a) and the S'S junction in Fig. 7(b). Since the energy gap $\Delta(x)$ decays to zero in Fig. 7(a)-(b), there are regions of local 'gapless' superconductivity near the NS interface where $v_s > \Delta(x)/p_F$. However, these regions of local 'gapless' superconductivity do not affect bulk properties such as critical current, critical temperature, etc. Since our self-consistent model shows that the supercurrent is approximately constant throughout the superconductor, depairing will occur when $v_s = v_d$ everywhere in the superconducting wire.

A different type of 'global' gapless superconductivity has been discussed by Sanchez and Sols⁴. In this proposed gapless superconductor⁴, a superconducting wire in contact with an NS junction is postulated to exist when $v_s > v_d$. It is true that such a non-equilibrium self-consistent solution to the BdG equations with $v_s > v_d$ does exist for a uniform superconducting wire. However, connecting such a wire in this novel 'global' gapless superconducting state to an NS junction imposes the additional constraint that the self-consistency condition in Eq. (21) must be satisfied at every point in space. When Eq. (21) is satisfied, the magnitude of the order parameter can no longer be a constant in space, as required for the globally gapless solution proposed in Ref.⁴ to exist.

Another way to view the situation proposed in Ref.⁴ is that, for a given applied voltage, the constraint of current conservation fixes both $\Delta(x)$ and v_s , leaving no

more degrees of freedom. The order parameter $\Delta(x)$ and superfluid velocity v_s cannot be adjusted independently as required for the bulk solution of Ref.⁴ to exist in an NS junction. Our self-consistent model shows instead that the ordering parameter of the superconducting wire collapses when the junction voltage is approximately $eV = \Delta$, or equivalently when $v_s = v_d$. In short, we see no possible way to achieve the non-equilibrium conditions necessary for this novel gapless superconducting state of Ref.⁴ to exist by connecting a superconducting wire to a ballistic NS junction. Fortunately, many other interesting measurements are possible at ballistic NS interfaces without invoking the global gapless superconducting state of Ref.⁴. In particular, the excess current larger than the point contact limit, which we find in section II, in no way depends on the gapless state proposed in Ref.⁴.

IV. CONCLUSIONS

It is possible to experimentally observe excess currents larger than the $(4/3)(2e\Delta/h)$ found for ballistic NS point contacts. By varying the width W_S of a superconducting wire in contact with a normal metal having width W_N , one can vary the effect of the supercurrent on the energy bands in the superconductor. Varying the widths of the two conductors controls the ratio of the number of conducting modes $\alpha \simeq W_S/W_N$ in the ballistic NS junction. We find the excess current attains a theoretical maximum of $(7/3)(2e\Delta/h)$ when $\alpha \simeq 7/3$. For $1 < \alpha < 7/3$ it should be possible to observe discontinuities in the I-V relation of the NS junction when the superfluid velocity v_s exceeds the Landau depairing velocity v_d . Although these results follow from a simple model which treats all conducting modes as equivalent, we confirmed the qualitative results using a more realistic model which includes the different supercurrent carried in each conducting mode and the scattering between the different modes. These predictions are based on a 'two-fluid' solution of the BdG equations, in which current conservation is violated locally near the NS interface.

To confirm our that our 'two-fluid' type treatment of the superfluid flow in NS junctions generates qualitatively accurate predictions for the I-V relations, we solved the BdG equations self-consistently for a single mode NS junction under an applied bias. Current conservation follows automatically in this self-consistent scheme, and shows that the superfluid velocity is indeed constant throughout the NS junction. The two important features confirmed in this self-consistent solution are (1) the superfluid velocity and terminal currents are the same as required by our 'two-fluid' scheme and (2) the order parameter indeed collapses when the superfluid velocity v_s equals the depairing velocity v_d . We did not perform a completely self-consistent calculation for the multiple moded NS junction, as we believe all the essential ele-

ments of this problem (so far as the excess current is concerned) are encompassed in the two-fluid treatment of the multiple-moded NS junction.

Having obtained the a self-consistent solution of the BdG equations for an NS junction under bias also enabled us to study the pair correlation function $F(x)$, order parameter $\Delta(x)$, and local density of states $N(x, E)$ in the NS junction. The peak near the superconducting energy gap at $E = \Delta$ in local density of states $N(x, E)$ inside the superconductor is split by the superfluid flow, as can be measured using STM spectroscopy. If the electron-phonon interaction in the normal metal is nearly zero, the density of states in the normal metal is unaffected by the presence of the superconductor. If the normal metal N is a weak superconductor held above its transition temperature, the STM can also measure changes in the local density of states $N(x, E)$ inside the normal metal. Due to the uniform superfluid velocity inside an NS junction, and the reduction of the order parameter near the NS interface, the Landau depairing condition is locally violated and a type of gapless superconductivity occurs locally near the NS interface.

V. ACKNOWLEDGMENTS

We thank Supriyo Datta for many useful discussions. We gratefully acknowledge support from the David and Lucile Packard Foundation and from the MRSEC of the National Science Foundation under grant No. DMR-9400415 (PFB).

VI. APPENDIX: DETERMINING THE SUPERFLUID FLOW VELOCITY

If the pairing potential and electron wavefunctions are determined from a self-consistent solution of the BdG equations, (1) electrical current will be conserved everywhere in space and (2) the superfluid flow will develop naturally as the scheme evolves towards self-consistency (c.f. section III). In this appendix we examine a different ‘globally self-consistent’ scheme, where current conservation is only guaranteed at the device leads. In this scheme, the correct value of the superfluid velocity $v_S = \hbar q/m$ is determined by equating the current operator evaluated on the normal side of the NS junction with the same operator evaluated deep (several coherence lengths) inside the superconductor. We then adjust the superfluid velocity (which is a free parameter in the scheme) until the current flowing out of the superconducting lead is the same as the current flow in the normal lead. We consider only a single moded NS junction with $M_N = M_S = 1$, although the results here are easily generalized to multiple conducting modes.

The derivation of the electrical current in Ref.¹² applies for an NS junction subject to a superfluid flow. Evaluating the current operator inside the normal region, Ref.¹² finds the well known formula developed by BTK¹¹, namely

$$I = (2e/h) \int_{-\infty}^{\infty} [1 - T_{Ne,Ne}(E) + T_{Nh,Ne}(E)] [f(E - eV) - f(E)] dE. \quad (29)$$

Here we use the notation of Ref.¹², where $T_{Ne,Ne} = R_N$ and $T_{Nh,Ne} = R_A$ are the particle current reflection probabilities for an electron-like quasi-particle incident from the normal metal (right index, ‘Ne’) to transmit as a hole or electron in the normal metal (left index). The sum rule from Eq. (4) then gives $I = I_{QP} + I_A$, with

$$I_{QP} = (2e/h) \int_{-\infty}^{\infty} [T_{Se,Ne}(E) - T_{Sh,Ne}(E)] [f(E - eV) - f(E)] dE, \quad (30)$$

and

$$I_A = (2e/h) \int_{-\infty}^{\infty} [T_{Nh,Ne}(E) + T_{Sh,Ne}(E)] [f(E - eV) - f(E)] dE. \quad (31)$$

To evaluate the electrical current operator inside the superconductor, we first note that the energy bands inside superconductor subject to a superfluid flow are⁸

$$\frac{\hbar^2 k^2}{2m} + \frac{\hbar^2 q^2}{2m} - \mu = \pm \sqrt{(E \mp \hbar^2 k q/m)^2 - |\Delta|^2}. \quad (32)$$

The discussion in Ref.⁸ can be extended to show that the particle current incident from the superconductor $J_P = (1/\hbar)(dE/dk)$. Thus, the particle current incident from the superconductor per unit energy is simply $1/\hbar$. Quasi-particles incident from the superconductor will then carry an electrical current of the form

$$I = \frac{e}{h} \int dE \frac{J_P^{\text{out}}}{J_P^{\text{in}}} \frac{J_Q^{\text{out}}}{J_P^{\text{out}}}. \quad (33)$$

We recognize the particle current transmission coefficient in Eq. (33) as

$$T_{\text{out,in}} = \frac{J_P^{\text{out}}}{J_P^{\text{in}}}. \quad (34)$$

To evaluate the $J_Q^{\text{out}}/J_P^{\text{out}}$ term in Eq. (33) we use several results from Ref.⁸. The scattering states inside the superconductor have solutions of the form

$$\begin{pmatrix} u(x) \\ v(x) \end{pmatrix} = \begin{pmatrix} u_{kq} \exp(iqx) \\ v_{kq} \exp(-iqx) \end{pmatrix} e^{ikx}. \quad (35)$$

The electrical current carried by each occupied state is therefore

$$J_Q = \left(\frac{\hbar k}{m}\right) (|u_{kq}|^2 + |v_{kq}|^2) f + \left(\frac{\hbar q}{m}\right) (|u_{kq}|^2 - |v_{kq}|^2) f, \quad (36)$$

and the particle current for each occupied state is

$$J_P = \left(\frac{\hbar k}{m}\right) (|u_{kq}|^2 - |v_{kq}|^2) f + \left(\frac{\hbar q}{m}\right) (|u_{kq}|^2 + |v_{kq}|^2) f. \quad (37)$$

The state are normalized so that $|u_{kq}|^2 + |v_{kq}|^2 = 1$. Hence the factor

$$\frac{J_Q^{\text{out}}}{J_P^{\text{out}}} = \frac{1}{(|u_{kq}|^2 - |v_{kq}|^2) + (q/k)} + \frac{(q/k)(|u_{kq}|^2 - |v_{kq}|^2)}{(|u_{kq}|^2 - |v_{kq}|^2) + (q/k)}. \quad (38)$$

The first term in Eq. (38) one can show is simply the ratio of the density of states in the superconductor to that of the normal metal (for a fixed value of wavevector k , not a fixed energy), namely

$$\tilde{N}^S(E) \equiv \frac{N_S(k)}{N_N(k)} = \frac{1}{(|u_{kq}|^2 - |v_{kq}|^2) + (q/k)}. \quad (39)$$

We make the translation between wavevector k and energy E inside the superconductor using Eq. (32). The second term in Eq. (38) will be only a minor correction to the first, being nearly zero near the Fermi level, equal to $(q/k) \ll 1$ over most of the energy range, and equal to 1 only near the bottom of the electron energy bands. The first term in Eq. (38) therefore dominates, being much larger than 1 near the Fermi level and equal to 1 over most of the energy range.

Applying the procedure outlined in Ref.¹² for construction of the scattering states, and multiplying by their appropriate Fermi occupation factors, we find a total current inside the superconductor of

$$I_S = I_1 + I_2. \quad (40)$$

The current I_1 arises from first term in Eq. (38) and is

$$\begin{aligned} I_1 = & \frac{2e}{h} \int_{-\infty}^{\infty} [\tilde{N}_{S_{e,out}}^S(E) T_{S_{e,Ne}}(E) - \tilde{N}_{S_{h,out}}^S(E) T_{S_{h,Ne}}(E)] [f(E - eV) - f(E)] dE \\ & + \frac{2e}{h} \int_{-\infty}^{\infty} \tilde{N}_{S_{e,out}}^S(E) [2f(E) - 1] dE - \frac{2e}{h} \int_{-\infty}^{\infty} \tilde{N}_{S_{e,in}}^S(E) [2f(E) - 1] dE. \end{aligned} \quad (41)$$

To obtain Eq. (41) we used the sum rule and electron hole symmetry, Eqs. (C.1) and (C.6) of Ref.¹². We distinguish between $\tilde{N}_{S_{h,out}}^S(E)$ and $\tilde{N}_{S_{e,in}}^S(E)$ in Eq. (41), since the incoming and outgoing electron-like quasi-particles have different densities of states. The second term in Eq. (38) results in a small correction current I_2 , proportional to (q/k_F) . The rather cumbersome expression for I_2 is

$$\begin{aligned} I_2 = & \frac{2e}{h} \int_{-\infty}^{\infty} [(q/k)(|u_{kq}|^2 - |v_{kq}|^2)]_{S_{e,out}} \tilde{N}_{S_{e,out}}^S(E) T_{S_{e,Ne}}(E) [f(E - eV) - f(E)] dE \\ & - \frac{2e}{h} \int_{-\infty}^{\infty} [(q/k)(|u_{kq}|^2 - |v_{kq}|^2)]_{S_{h,out}} \tilde{N}_{S_{h,out}}^S(E) T_{S_{h,Ne}}(E) [f(E - eV) - f(E)] dE \\ & + \frac{2e}{h} \int_{-\infty}^{\infty} [(q/k)(|u_{kq}|^2 - |v_{kq}|^2)]_{S_{e,out}} \tilde{N}_{S_{e,out}}^S(E) [2f(E) - 1] dE \\ & - \frac{2e}{h} \int_{-\infty}^{\infty} [(q/k)(|u_{kq}|^2 - |v_{kq}|^2)]_{S_{e,in}} \tilde{N}_{S_{e,in}}^S(E) [2f(E) - 1] dE. \end{aligned} \quad (42)$$

We again translate between k and E inside the superconductor using Eq. (32), taking care to assign the appropriate branch of the dispersion curve for incoming or outgoing electron- or hole- like particles. The first two terms in I_2 are a small correction to the superfluid flow due to additional quasi-particle injection, while the last two terms are a small correction to the equilibrium superfluid flow. A rigorous treatment guaranteeing global current conservation at any temperature would equate the current I from Eq. (29) with the current I_S from Eq. (40), adjusting the superfluid velocity q until $I = I_S$.

We now analyze the validity of our ‘two-fluid’ procedure from Section II. We henceforth neglect the current I_2 as insignificant compared with I_1 . At zero temperature, the current operator evaluated inside the superconductor we find from Eq. (41) as

$$I_1(T=0) = \frac{2e}{h} \int_0^{eV} [\tilde{N}_{Se,out}^S(E) T_{Se,Ne}(E) - \tilde{N}_{Sh,out}^S(E) T_{Sh,Ne}(E)] dE + \frac{4e\Delta}{h} (v_s/v_d). \quad (43)$$

The zero temperature limit of Eq. (29) is given in Section II as Eqs. (6)-(7). The second term in Eqs.(43) is the superfluid flow term I_C . So we can certainly identify I_A from Eq. (7) with I_C . However, Eq. (6) for I_{QP} is not exactly equal to the first term in Eq. (43), the difference being the additional factor of the superconducting density of states $\tilde{N}^S(E)$ in Eq. (43).

For the Cooper pair flow away from the NS interface (which we are considering in this paper), and for the energy range between 0 and eV , the outgoing hole-like quasi-particle conduction channel opens at a lower energy than the electron-like quasi-particle channel (see Fig. 2). This means the first term in Eq. (43) will be larger and more negative than I_{QP} from Eq. (7), requiring a larger value of the superfluid velocity v_s at each value of the applied voltage V than in the two-fluid model of Section II. We conclude that the treatment in Section II therefore underestimates the effect of superfluid flow on the excess current.

¹ A.F. Andreev, ‘The Thermal Conductivity of the Intermediate State in Superconductors’, Zh. Eksp. Teor. Fiz. **46**, 1823 (1964). [Sov. Phys. JETP **19**, 1228 (1964).]

² R. Kummel, ‘Dynamics of Current flow Through the Phase-Boundary Region between a Normal and a Superconducting Region’, Z. Physik **218**, 472 (1969).

³ W.N. Mathews, ‘Quasiparticle, Charge, and Energy Conservation in Weak-Coupling Superconductors’, Phys. Stat. Sol.(b), **90**, 327 (1978).

⁴ J. Sanchez-Canizares and F. Sols, ‘Self-consistent current-voltage characteristics of normal-superconductor interfaces’, J Phys. Condens. Matt.**5**, L301 (1996).

⁵ J. Sanchez-Canizares and F. Sols, ‘Self-consistent scattering description of transport in normal-superconductor structures’, Phys. Rev. B **55**, 531 (1997).

⁶ A. Martin and C.J. Lambert, ‘Self-consistent current-voltage characteristics of superconducting nanostructures’, Phys. Rev. B **51**, 17999 (1995).

⁷ L. Chang, S. Chaudhuri, and P.F. Bagwell, ‘Critical current of a Quasi-one-dimensional Superconducting Wire’, Phys. Rev B, **54**, (1996).

- ⁸ P.F. Bagwell, ‘Critical Current of a One-Dimensional Superconductor’, Phys. Rev B, **49**, 6841 (1994).
- ⁹ R.A. Riedel L. Chang, P.F. Bagwell, Phys. Rev. B, ‘Critical current and self-consistent order parameter of a superconductor-normal-metal-superconductor junction’, **54**, 16082 (1996).
- ¹⁰ S. Hoffman and R. Kummel, ‘Ehrenfest theorem for inhomogeneous superconductors and supercurrent force on Andreev reflected quasiparticles’, Z. Phys. B - Condens. Matt. **84**, 237 (1991).
- ¹¹ G.E. Blonder, M. Tinkham, T.M. Klapwijk, ‘Transition from Metallic to Tunneling regimes in superconducting Microconstrictions’, Phys. Rev. B., **25** 4515, (1982).
- ¹² S. Datta, P.F. Bagwell, and M.P. Anantram, ‘Scattering Theory of Transport for Mesoscopic Superconductors’, Physics of Low Dimensional Structures, **3**, 1 (1996).
- ¹³ L. Landau, ‘The Theory of Superfluidity of He II’, J. of Phys. (USSR), **5**, 71 (1941).
- ¹⁴ C.J. Pethik and H. Smith, ‘Relaxation and Collective Motion in Superconductors: A two-fluid description’, Ann. Phys., **119**, 133 (1979).
- ¹⁵ R.A. Riedel, Ph.D. Thesis, Purdue University, 1997.
- ¹⁶ P.G. de Gennes, *Superconductivity of Metals and Alloys* (Benjamin, New York 1966).
- ¹⁷ F. Sols and J. Ferrer, ‘Crossover From the Josephson Effect to Bulk Superconducting Flow’, Phys. Rev. B, **49**, 15913 (1994).
- ¹⁸ A. Furusaki and M. Tsukada, ‘DC Josephson Effect and Andreev Reflection’, Solid State Communications, **78**, 299 (1991).
- ¹⁹ M. Hurd, S. Datta, and P.F. Bagwell, ‘ac Josephson effect for asymmetric superconducting junctions’, Physical Review B-1, **56**, 11232 (1997).
- ²⁰ W.L. McMillan ‘Theory of Superconductor-Normal-Metal Interfaces’, Phys. Rev., **175**, 559 (1968).
- ²¹ D.S. Falk, ‘Superconductors with Plane Boundaries’, Phys. Rev. **132**, 1576 (1963).
- ²² A.C. Mota, P. Visani, and A. Pollini, ‘Magnetic Properties of Proximity-Induced Superconducting Copper and Silver’, J. Low Temp. Phys., **76**, 465 (1989)
- ²³ S.H. Tessmer, D.J. van Harlingen, and J.W. Hyding, ‘Observation of Bound Quasiparticle States in Thin Au Islands by Scanning Tunneling Microscopy’, Phys. Rev. Lett. **70**, 3135 (1993).